Chemical Papers (2023) 77:5979–5988
https://doi.org/10.1007/s11696-023-02914-0

ORIGINAL PAPER

Utility of eco-friendly microwave-assisted nitrogen-doped carbon dots as a luminescent nano-sensor for the ultra-sensitive analysis of tigecycline in dosage form and biological samples

Baher I. Salman[1]

Received: 24 January 2023 / Accepted: 4 June 2023 / Published online: 13 June 2023
© The Author(s) 2023

Abstract

In the presented work, simple, green, sensitive, and selective nitrogen-doped carbon quantum dots (N-CQDs) were developed as nano-sensor for quantification of tigecycline (TIG) in different matrices. The proposed method is based on microwave synthesis of green nitrogen-doped carbon quantum dots with a high quantum yield (41.39%) and size diameter equal to 2.0 nm from the green juice of *Eruca sativa* leaves. The relative fluorescence intensity (RFI) of the green synthesized quantum dots (N-CQDs) was quenched at emission 512 nm (excitation 445 nm) after the addition of TIG drug. A good linear range between TIG concentration and quenched fluorescence intensity of N-CQDs in the range 20–300 ng mL^{-1}, with the lower limit of quantitation (LOQ) equal to 8.51 ng mL^{-1}. The proposed method was validated using the international conference of harmonization (ICH) recommendation and bio-analytical validation using U.S. food and drug administration (US-FDA) guidelines. The N-CQDs have been fully characterized using a transmission electron microscope (TEM), dynamic light scattering (DLS), X-Ray photoelectron spectroscopy (XPS), and Fourier-transform infrared spectrometer (FTIR). The suggested technique is a straightforward analytical procedure that can be used in clinical laboratories. Under the optimum condition, TIG was estimated in human plasma with a high percentage of recovery ranging from 96.95 to 98.54%. In addition, the proposed method was applied effectively in milk samples with percentage of recovery equal to 98.90 ± 1.55.

Keywords Tigecycline · Plasma · Vial · N-CQDs · Fluorimetry · Milk

Introduction

Tigecycline (TIG) is a broad-spectrum antibiotic drug. TIG was prescribed for the treatment of various infectious diseases such as community-acquired pneumonia and skin disease. Community-acquired pneumonia is one of the most common infectious diseases with high mortality and morbidity worldwide. Spreading infectious diseases is the most reason for the need for innovative new antibiotics for bacterial resistance like Streptococcus pneumoniae and Hemophilus influenzae to beta-lactams, macrolides, and earlier generations of tetracyclines· (Honeyman et al. 2015; McKeage et al., 2008; Villano et al. 2016).

TIG, Fig. 1a is [4S-(4α,4aα,12aα)]-4,7-Bis(dimethylamino)–9–[2-(1,1-diethylethyl)acetlyamino]-1,4,4a,5,5a,6,11,12a-octahydro-3,10,12,12atetrahdroxy1,11-dioxo-2-naphthacene carboxamide.

Few strategies have been described for the examination of TIG since it is just available on the market, these techniques are spectrophotometric (Magalhães da Silva et al. 2012), fluorometric (Ge et al. 2015; Molina-García et al. 2011; Salman et al. 2019), and chromatographic approaches (Ji et al. 2008; Ji Ji et al. 2010).

Major limitations were observed in previously published techniques that evaluate TIG as suffering low sensitivity and lack of bio-analytical proofs (Ge et al. 2015; Magalhães da Silva et al. 2012; Molina-García et al. 2011), the demand for sophisticated and expensive equipment's, availability for the utilization and disposal of solvents and individuals experienced in these technologies (Ji et al. 2008; Ji Ji et al. 2010). Due to their simplicity, low cost, specificity, and widespread availability in most quality control laboratories, spectrofluorimetric approaches are among the most common

✉ Baher I. Salman
bahersalman@azhar.edu.eg; bahersalman2013@yahoo.com

[1] Pharmaceutical Analytical Chemistry Department, Faculty of Pharmacy, Al-Azhar University, Assiut branch, Assiut 71524, Egypt

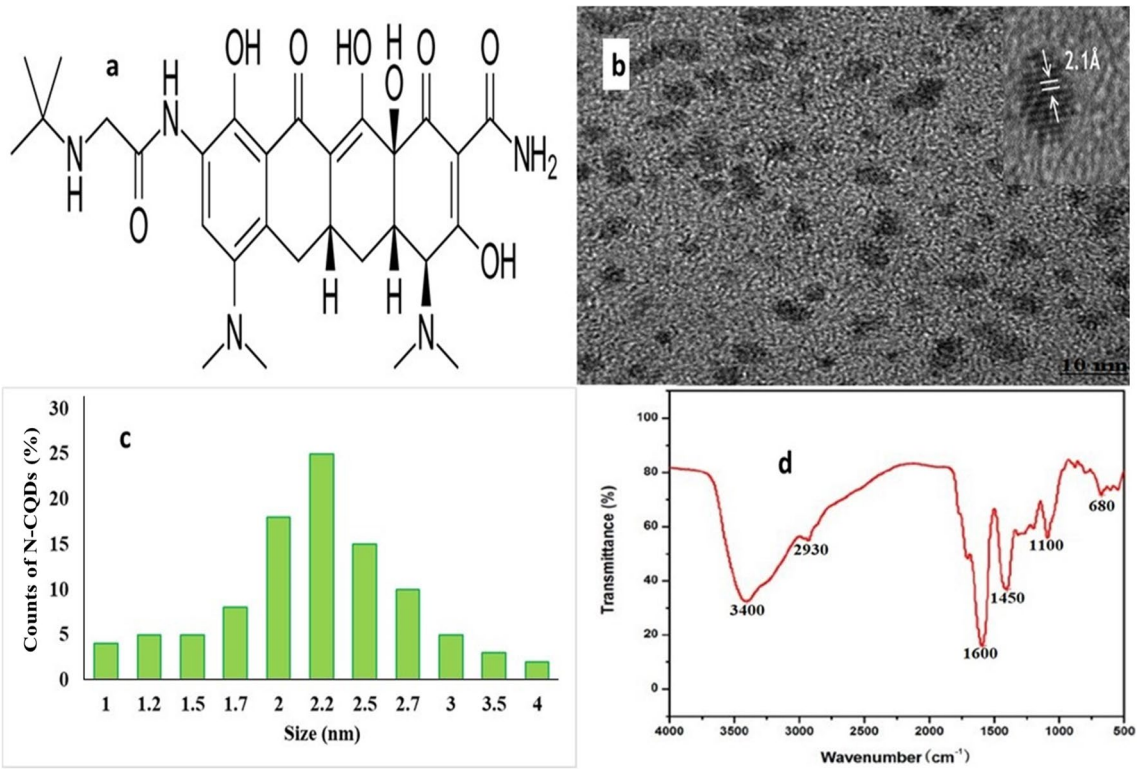


Fig. 1 **a** Chemical structure of TIG, **b** Transmission electron microscope image of nitrogen-dopped carbon quantum dots, **c** Dynamic light scattering image for synthesized green N-CQDs and **d** FTIR spectroscopy for N-CQDs

and sensitive techniques (Hammad et al. 2017; Salman et al. 2023; Salman et al. 2022a, b, c). The last ten years have seen a strong development of quantum dots (QDs), which have distinct optical features, excellent water solubility, biocompatibility, non-toxicity, and ease of functionalization.

Novel quantum dots are currently seen as a great alternative to fluorescent dyes and fluorescence derivatizing agents because of their exceptional and adaptable fluorescence properties. Compared to metal-based nanoparticles, they also are less toxic and hazardous to the environment (M. F. B. Ali et al. 2023; Salman et al. 2022a, b, c; Salman et al. 2022a, b, c). Additionally, diverse processes such as dry heat, hydrothermal, and solvothermal approaches were used to create carbon quantum dots (CQDs). These techniques have several shortcomings, however, as they go against the notion of "green chemistry," taking up to 24 h, requiring temperatures of 300 degrees, and utilizing harsh chemicals and organic solvents (Wang et al. 2019). Microwave synthesis is a revolutionary technique that has recently been applied to create high-yield quantum dots while reducing the synthesis period from hours to minutes. (Choi et al. 2017; Eskalen et al. 2020).

Eruca sativa plants are frequently grown in Egypt and have very affordable leaves. It is the first leaf vegetable that humans have ever eaten. The leaves of the *Eruca sativa* plant are a rich source of several nutrients and vitamins, including sugar, fiber, carbs, vitamin A, vitamin B1, riboflavin, glycosides and folic acid (Hussein 2013; Miyazawa et al. 2002; Neriman et al. 2011).

We subsequently created an integrated strategy for greening both the synthesis processes and the source of carbon to restore the greenness and sustainability of the synthesis of N-CQDs. The suggested technique only employs low-power microwave-assisted synthesis for 4 min at 700 W. We also have access to affordable, abundant, and practical flora. The study's environmental friendliness is also in line with broad claims about green chemistry and security.

Experimental section

Materials and reagents

All the chemicals and materials used in this work were of high purity and analytical grade. Tigecycline (TIG) 99.9% and Tigacyl® vial (50 mg) were provided from Pfizer, Cairo, Egypt. Egyptian Blood Bank provided human plasma samples, which were then kept in storage at − 24 °C until processing.

The standard solution of TIG (100 µg mL^{-1}) was prepared by dissolving 10 mg TIG powder in 100 mL distilled water. The working standard solution was prepared by serial dilution with distilled water to obtain a concentration range (0.2—3.0 µg mL^{-1}).

Instrumentation of the N-CQDs approach

An FS5 spectrofluorometer was used to collect the data and a 150 W xenon lamp. Moreover, it is coupled to the Fluoracle® software and has a 1-cm quartz cell, and the slit widths were 2 nm (Edinburgh, UK). The dynamic light scattering measurements (DLS) were scanned by the Zetasizer Red badge instrument of ZEN 3600 Nano ZS model (Malvern, UK). High-resolution transmission electron microscope (TEM) JEOL JEM-100CX II with tungsten EM filament 120 (USA).

The MFMI-100A microwave device was created to facilitate solvent extraction and chemical synthesis (MED Future). IR Temperature Sensor with magnetic and mechanical stirring from 100 to 1500 rpm (Australia). A Fourier-transform infrared (FTIR) spectrometer was utilized to determine the functional groups of the quantum dots (Germany). A Philips X-ray diffractometer was used to scan the powder X-ray diffraction (PXRD). Benchtop pH meter (100 B, China). Unicen 21 centrifuges with a speed 10.000 rpm (Spain).

Synthesis of nitrogen green quantum dots

The green nitrogen-doped carbon quantum dots were synthesized using thermolysis of *Eruca Sativa* leaves. The leaves were crushed well and filtrated, then 40 mL of the filtrate was transferred into the reaction vessel and then placed in the microwave. Microwave source: 2450 MHz, 700 W for 4 min until a brown solution was formed. The residue was dispersed in 50 mL ultra-pure water and then sonicated for 30 min to remove large particles. The solution was filtered and centrifuged at 4000 rpm for 10 min. the supernatant was filtrated via 0.45 µm cellulose membrane. The obtained yellow filtrate color solution was utilized for the experiment.

The fluorimetric procedure of TIG

In a 10-mL volumetric flask, one milliliter of N-CQDs (0.17 mg mL^{-1}) was added together with one milliliter of Britton-Robinson (BR) buffer (pH 6.6). Next, 1.0 ml of the different concentrations of the standard working solution of TIG was added in the range (0.2 – 3.0 µg mL^{-1}). The solution was completed to the mark via ultrapure water to obtain the final concentration range (20 – 300 ng mL^{-1}). After 8 min, the relative fluorescence intensity (RFI) was scanned at 512 nm (excitation 445 nm).

Estimation in pharmaceutical product

Tigacyl® vial (50 mg TIG) was analyzed by an equivalent amount equal to (10.0 mg) TIG put into a volumetric flask and dissolved in 100 mL of ultrapure water, to obtain a concentration of 100 µg mL^{-1}.

Preparation of spiked plasma

A sufficient amount of TIG solution was added to 0.5 mL of human plasma before being spiked into a centrifuge tube. the protein precipitating agent acetonitrile was then added for a total of 1 mL (Omar et al. 2016; Salman et al. 2019). After 30 s of vertexing, the fluid was diluted to 10 mL. The product was centrifuged for 30 min. at 3500 rpm, and 1.0 mL of the supernatant was then employed in the analysis.

Preparation of milk sample

The milk sample (0.5 mL) was combined with 1.0 mL of acetonitrile, TIG was added, and the mixture was shaken for 30 s. The mixture was centrifuged for 10 min at 3500 rpm after being sonicated for 5 min. The supernatant was then removed for further examination (H. R. H. Ali et al. 2021). The Drug-free milk samples were prepared using the same steps without the addition of TIG.

Measurement of the accuracy and replication

The accuracy of the N-CQDs technique was studied using various concentrations from TIG (30, 50, 100.0, 200, and 300.0 ng mL-1) within the calibration range was used.

Moreover, the precision of the N-CQDs method was further tested using three replicates of each concentration (100.0, 150.0, and 250.0 ng mL^{-1}).

Results and discussion

Characterization of N-CQDs

The N-CQDs have been fully characterized using a high-resolution transmission electron microscope (TEM), X-Ray photoelectron spectroscopy (XPS), Zeta potential analysis, fluorescence, UV–VIS, and FT-IR spectroscopy. A high-resolution transmission electron microscope (TEM) was used to analyze the surface morphology of N-CQDs. The size was found to be 2.0 ± 0.1 nm (Fig. 1b). The size of the N-CQDs was confirmed using dynamic light scattering (DLS). It was observed that the size was found to be 2.2 ± 0.1 nm, which is compatible with the TEM image (Fig. 1c). The functional groups on the exterior surface of N-CQDs were investigated using FTIR spectroscopy, as shown in Fig. 1d.

The FTIR bands at 3400 cm^{-1} and 2930 cm^{-1}, respectively, indicate the function groups (-NH, -OH), and (-CH). The bands at 1600 and 1450 cm^{-1} demonstrate the -C = O and -C-N groups, respectively. Moreover, the peaks at 1100 cm^{-1} and 680 cm^{-1}, respectively, reflect N–O and C-O. (Fig. 1d) The research focuses on the synthesis of multifunctional nitrogen-doped quantum dots.

For the elemental analysis, X-Ray photoelectron spectroscopy (XPS) was also used. Three distinctive significant peaks at 284.9, 395.6, and 538.5 eV, which correspond to C 1 s, N 1 s, and O 1 s, were detected as the XPS peaks of N-CQDs. It means that the main components of C-dots are O (43.00%), C (37.89%), and N (19.11%), as shown in Fig. S1a (supplementary materials). There are 4 peaks in the C1s spectra (Fig. S1b), which correspond to the existence of the C = C, C-N, C-O, and C = O groups, respectively. For N1s spectrum, 2 peaks are observed at 399.2 eV and 400.8 eV, produced due to the presence of C-N and N–H as shown in Fig. S1c (Ghosh et al. 2021). For O1s spectrum has two peaks for C–OH, C–O–C, and C = O at 531.4 eV and 532.6 eV (Fig. S1d) (Jothi et al. 2021; Salman et al. 2022a, b, c). The quantum dot morphological characteristics show that the structure of N-CQDs contains multiple functional groups (-NH2, -OH, COO-), which interpret the interaction between TIG and N-CQDs via electrostatic interaction and hydrogen bonding. The energy-dispersive X-ray spectrometer (EDX), as depicted in Fig. S2, was used to check for the existence of the elements (C, N, and O). The spectrum reveals the presence of the elements C, N, and O. Additionally, the peak shown at 24.60 is a diagnostic peak of carbon dots (Salman et al. 2022a, b, c; Salman et al. 2022a, b, c), which was observed in Fig. S3 of the powder X-ray diffraction (PXRD) picture used to analyze the generation of N-CQDs.

The quantum yield of N-CQDs

The proposed method provides high quantum yield due to reducing the sizes of N-CQDs (2.0 nm) would increase the quantum yields by creating more optical effects via an increasing number of functional groups on the surface of quantum dots as described in Fig. 1d (Bae et al. 2008; Yang et al. 2016). Additionally, Eruca Sativa leaves are abundant in several elements and vitamins, such as carbohydrates, sugar, fibers, vitamin A, vitamin B1, riboflavin, and folic acid, which resulted in a wide range of functional groups during the production of quantum dots.

The quantum yield (QY) of N-CQDs was studied via single point method using the following equation (Salman et al. 2022a, b, c; Salman et al. 2022a, b, c; Salman et al. 2022a, b, c):

$$Q_{NCQDs} = Q_{Quinin} x \frac{F_{NCQDs}}{F_{Quinin}} \text{x} \frac{A_{st}}{A_{NCQDs}} \text{x} \frac{\eta^2(NCQDs)}{\eta^2(Quinin)}$$

Q is the quantum yield, while F is integrated fluorescence. The quantum yield of nitrogen quantum dots was found to be = 41.39%.

Optical characterization of N-CQDs

As shown in Fig. 2a, the UV spectrum of quantum dots displays a characteristic absorption peak at 225 nm, which is principally derived from the π-π* transition of carbonaceous skeleton, and at 295 nm for n- π* electronic transition of C = O and C = C which represented in Fig. 1d (Ali et al. 2019).

When the excitation wavelengths used to scan the relative fluorescence spectra of N-CQDs were increased, the

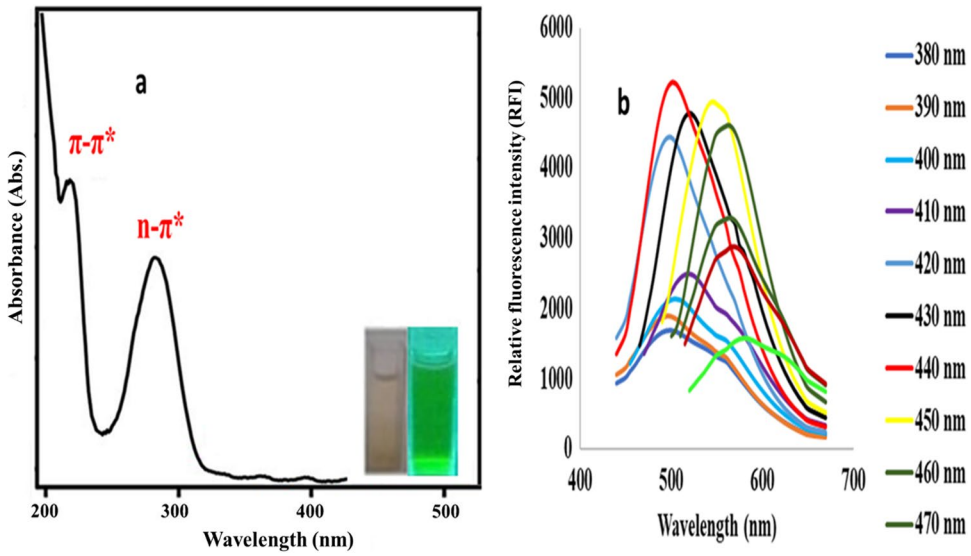


Fig. 2 **a** UV spectrum of optical characters of N-CQDs and **b** Excitation dependent emission spectra of N-CQDs

emission spectra of the N-CQDs shifted toward the red, from 380 to 470 nm, and the RFI decreased, demonstrating the excitation-dependent emission of carbon dots (Salman 2023). Figure 2b

The reaction mechanism of TIG with N-CQDs

According to Fig. 3a, the fluorescence of nitrogen-doped carbon quantum dots gradually decreased as the TIG concentration increased at 512 nm.

The Stern–Volmer equation was used to evaluate the reaction mechanism between TIG and N-CQDs and distinguish between dynamic and static quenching using the following expression:

$$F0/F = 1 + Ksv\,[Q]$$

Ksv is the Stern–Volmer constant, Q is TIG concentration, and F0 and F are fluorescence in the absence and presence of TIG.

The linearity of the Stern–Volmer curve, as seen in (Fig. 3b), clearly indicates that the quenching process is dynamic. Excited N-CQDs interact with TIG, resulting in an energy/electron transfer and a reduction in the fluorescence of the quantum dots. This mechanism is properly described by the Stern–Volmer model (Fig. 3b).

Stern–Volmer equations at various temperatures were used to confirm dynamic quenching. According to the Stern–Volmer plots (Fig. 3c), dynamic quenching rises as temperature rises (Larsson et al., 2022; Magdy et al. 2022).

Moreover, the presence of multiple functional groups in TIG permits the formation of hydrogen bonds and electrostatic attraction among TIG and nitrogen-doped carbon dots that have various functional groups as in Fig. 1d, in addition to allowing for these other phenomena. (Salman 2023; Salman et al. 2022a, b, c).

Optimization of the quantum dots method with TIG

In the presence of TIG, investigations into the effect of pH on N-CQD fluorescence were carried out. N-CQDs were shown

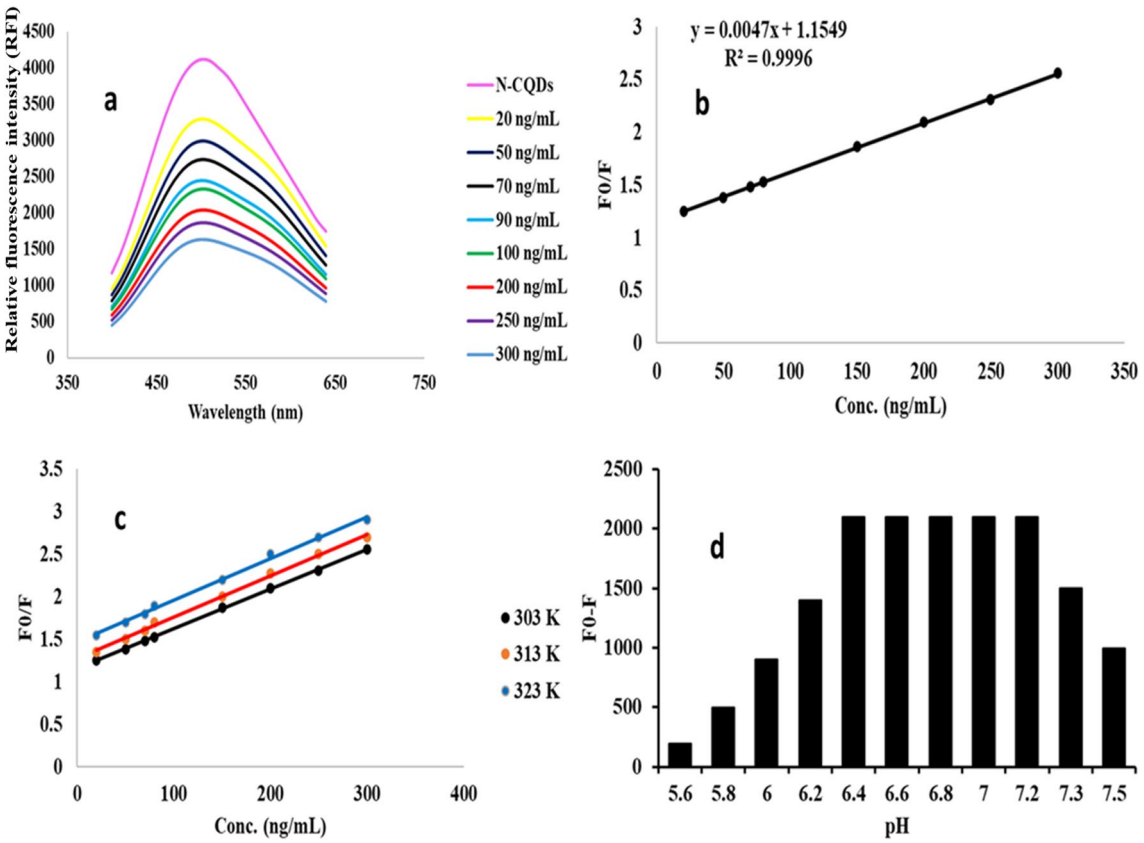


Fig. 3 **a** Reaction of N-CQDs with different concentrations of TIG, **b** Stern–Volmer curve between N-CQDs using different concentrations of TIG at room temperature F0 in absence and F in the presence of TIG, **c** Stern–Volmer curve between N-CQDs using different concentrations of TIG at different temperatures, and **d** Effect of pH on the reaction of TIG (100 ng mL^{-1}) with N-CQDs. *F0 is the relative fluorescence intensity of N-CQDs in absence of TIG. *F is the relative fluorescence intensity of N-CQDs in the presence of TIG

to quench continuously in the pH range of 6.4 to 7.2 due to the presence of several function groups confirmed via FTIR curve (Fig. 1d), however, raising the pH to 7.2 caused an unstable drop in RFI. Thus, it was determined that 6.6 was the ideal pH. Figure 3d

Additionally, multiple N-CQD concentrations were investigated during the reaction with TIG (100 ng mL^{-1}), and it was shown that the quenching produced at the concentration with the greatest stability was 0.17 mg mL^{-1} (1.0 mL) (Fig. 4a).

At various time intervals spanning from 0 to 30 min, the reactivity of TIG with N-CQDs in pure form was observed. Within 8 min, the greatest stable quenching was recorded (Fig. 4b).

The response of TIG with N-CQDs in pure form was noticed at various intervals ranging from 0 to 30 min. The maximum steady quenching was observed within 8 min (Fig. 4b).

The validation of TIG with the N-CQDs method

The proposed method for the reaction of TIG in the presence of N-CQDs under ideal conditions was validated using ICH and US-FDA standards (Branch 2005; Zimmer 2014). The green fluorescence of the created N-CQDs was quenched at 512 nm as the TIG concentration increased (excitation at 445 nm) (Fig. 3a).

The regression equation was identified as $Y = 0.0047x + 1.154$ using the Stern–Volmer equation; adequate linearity was found within the range of 20–300 ng mL^{-1}; and the correlation coefficient was 0.9996 (Fig. 3b).

The lower limit of detection (LOD) and limit of quantitation (LOQ) were calculated using the following equations:

$$\mathrm{LOQ} = 10\partial/\text{ slope}, \mathrm{LOD} = 3.3\partial/\text{ slope},$$

LOQ and LOD were found to be 8.51 and 2.80 ng mL^{-1}, respectively, the results refer to ultra-sensitivity of the N-CQDs method (Table 1).

To test the accuracy of the N-CQDs technique, various TIG drug concentrations (30, 50, 100.0, 200, and 300.0 ng mL-1) within the calibration range were used. The relative standard deviation (RSD) scores were obtained from 0.22 to 0.90 in Table 2, and recovery percentages ranged from 100.28 to 101.82%.

The precision of the N-CQDs method was further tested using three replicates of each concentration (100.0, 150.0, and 250.0 ng mL^{-1}). According to Table 2, the relative standard deviation ranged from 0.30 to 0.74%, showing the high reproducibility of the N-CQDs method.

Furthermore, by making minor changes to the analytical procedure's parameters, the robustness of the green synthesized N-CQDS for TIG estimation was used. A small adjustment to the procedure variables had no appreciable impact, as shown in Table S1 (Supplementary materials).

Three concentrations were used to conduct a bio-analytical validation of the reaction of TIG and N-CQDs in human plasma in compliance with US-FDA regulations (50, 100, and 250 ng mL^{-1}). The RSD value ranged from 1.55 to 2.60 in Table 3, and the results demonstrate that the N-CQDs approach in human plasma produces excellent accuracy.

As demonstrated in Table S2, the N-CQDs approach was also employed to research the stability of TIG in human plasma. The stability was examined under various conditions

Table 1 Analytical parameters for measuring TIG utilizing N-CQDs

Parameter	TIG
λ_{ex} (nm)	445
λ_{em}(nm)	512
Concentration range (ng mL^{-1})	20–300
Determination coefficient (r^2)	0.9996
Slope	0.0047
Intercept	1.154
SD the intercept (Sa)	0.004
LOD (ng mL^{-1})	2.80
LOQ (ng mL^{-1})	8.51

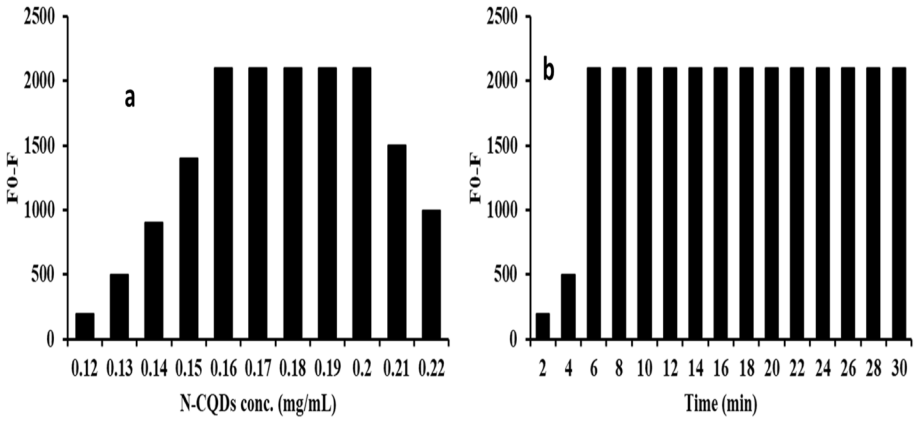


Fig. 4 **a** Effect of N-CQDs concentration on the reaction of TIG (100 ng mL^{-1}), and **b** Effect of the reaction time for the reaction of N-CQDs with of TIG (100 ng mL^{-1}). *F0 is the relative fluorescence intensity of N-CQDs in absence of TIG. *F is the relative fluorescence intensity of N-CQDs in the presence of TIG

Table 2 Quantum dots technique's accuracy and precision in estimating pure TIG

Sample number	Taken Conc (ng mL^{-1})	Found Conc (ng mL^{-1})	% Recovery * ± RSD
1	30.0	30.21	100.70 ± 0.43
2	50.0	50.14	100.28 ± 0.58
3	100.0	101.82	101.82 ± 0.22
4	200.0	200.74	100.37 ± 0.90
5	300.0	303.60	101.20 ± 0.60
Intra-day precision	100.0	102.11	102.11 ± 0.30
	150.0	150.90	100.60 ± 0.55
	250.0	253.44	101.37 ± 0.60
Inter-day precision	100.0	99.66	99.66 ± 0.74
	150.0	148.66	99.10 ± 0.43
	250.0	249.14	99.65 ± 0.39

*Average of three determinations

using three levels of low-quality controls (LQC), medium-quality controls (MQC), and high-quality samples (HQC). According to the results, TIG is stable in human plasma at diverse conditions. Table S2.

Quantification of TIG using the N-CQDs method in human plasma and milk samples

Due to the ultra-sensitivity of the N-CQDs approach, tigecycline (TIG) was successfully estimated in spiked human plasma. When using six different concentration levels, the recovery percentage for the studied procedure ranged from 96.95 to 98.54%. The analytical method's variability caused by various matrix effects was measured as the relative standard deviation (RSD), which ranged from 1.21 to 2.18 and is given in Table 4.

In addition, the proposed method was applied effectively for the estimation of TIG in milk samples. The results refer to the high sensitivity of the proposed method as in Table 4.

Quantification of TIG in commercial form

For quantifying TIG in market dosage form (Tigacyl® 50 mg vial), the suggested method (N-CQDs) was employed successfully. The percentage of recovery RSD discovered was 102.50 ± 1.11 when compared to the reported approach (Salman et al. 2019) (100.34 ± 1.11). The t-value was 1.34 and the F-value was 2.40, respectively.

Assessment of the greenness of the proposed method

Various methods have been recently observed for the evaluation of the greenness of the analytical methods. These methods are useful for the reduction of environmental pollution generated by analytical techniques such as chromatographic methods. AGREE and GAPI methods were utilized for the greenness assessment of the proposed method (Saraya et al. 2022). AGREE depicts a clock-shaped symbol with a perimeter divided into 12 pieces, each representing a GAC concept. The pictogram's center

Table 3 Matrix effect study for determination of TIG in human plasma

	Intra-day assay(n = 6)			Inter-day assay(n = 18)		
Conc. (ng mL^{-1})	Found (ng mL^{-1})	Accuracy (%)	Precision (CV %)	Found (ng mL^{-1})	Accuracy (%)	Precision (CV %)
50	48.60	97.20	1.66	48.20	96.40	2.60
100	97.14	97.14	2.21	96.66	96.66	2.33
250	246.11	98.44	2.30	245.20	98.08	1.55

Table 4 Quantification of TIG using N-CQDs in spiked human plasma and milk samples

Added conc (ng mL^{-1})	Human plasma		Milk samples	
	Found Conc (ng mL^{-1})	% Recovery * ± RSD	Found Conc (ng mL^{-1})	% Recovery * ± RSD
50	48.90	97.80 ± 1.66	49.10	98.20 ± 1.72
100	98.54	98.54 ± 1.21	98.90	98.90 ± 1.55
150	147.16	98.10 ± 1.79	148.30	98.86 ± 1.90
200	193.48	96.74 ± 2.18	196.48	98.24 ± 1.49
250	244 .49	97.79 ± 2.11	244 .80	97.92 ± 1.90
300	290.85	96.95 ± 1.44	293.44	97.81 ± 1.74

*Average of six determinations

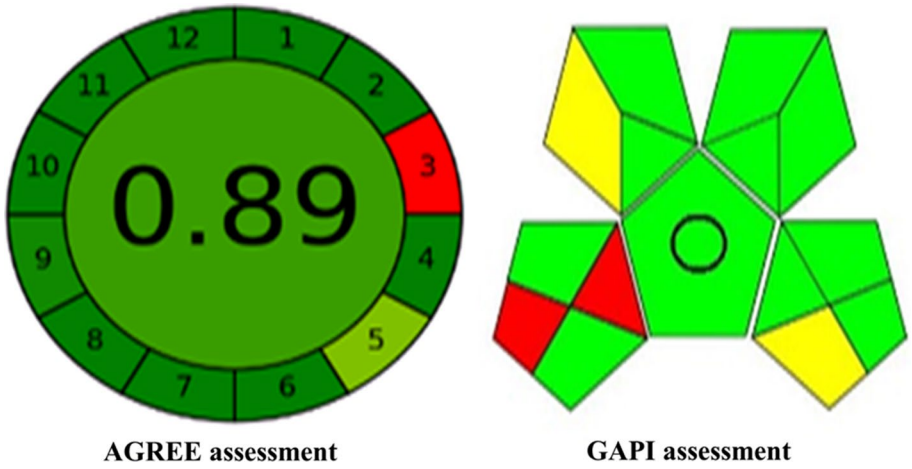


Fig. 5 Greenness assessment of the proposed method using AGREE and GAPI methods

displays a number value estimating the ecological impact, with the closer to one, the greater the damage as shown in Fig. 5. Moreover 2 red zones appear while using GAPI method (third and fourth) due to sample transportation and using acetonitrile as a protein precipitating agent (Fig. 5).

The results refer to the high greenness effect of the proposed method (N-CQDs) which agrees with the US climate change conference.

Conclusion

This work aims to establish a green fluorimetric approach using nitrogen-doped carbon quantum dots with high quantum yield. The N-CQDs method is a simple, environmentally friendly, highly sensitive, affordable, and rapid strategy used as a fluorescent probe for analysis of TIG. To quickly generate the N-CQDs, a one-pot, low-energy, chemical-free carbonization microwave assisted was used for the synthesis of quantum dots. The proposed technique was evaluated and bioanalytically validated following ICH and US-FDA guidelines. These N-CQDs were successfully used to determine TIG pharmaceutical dosage form, human plasma, and milk samples. As a result, this simple and label-free sensing technology was used for fluorescence-based analysis of the target analyte.

Supplementary Information The online version contains supplementary material available at https://doi.org/10.1007/s11696-023-02914-0.

Author contributions Conceptualization, Methodology, Formal analysis, Validation, Writing-review & editing of the manuscript were carried out by Baher I. Salman.

Funding Open access funding provided by The Science, Technology & Innovation Funding Authority (STDF) in cooperation with The Egyptian Knowledge Bank (EKB).

Data availability All data generated or analyzed during this study are included in this published article (and its supplementary information files).

Declarations

Conflict of interest The authors have no competing interests to declare that are relevant to the content of this article.

Ethics approval Not applicable.

Consent to participate Not applicable.

Consent to publish Not applicable.

Open Access This article is licensed under a Creative Commons Attribution 4.0 International License, which permits use, sharing, adaptation, distribution and reproduction in any medium or format, as long as you give appropriate credit to the original author(s) and the source, provide a link to the Creative Commons licence, and indicate if changes were made. The images or other third party material in this article are included in the article's Creative Commons licence, unless indicated otherwise in a credit line to the material. If material is not included in the article's Creative Commons licence and your intended use is not permitted by statutory regulation or exceeds the permitted use, you will need to obtain permission directly from the copyright holder. To view a copy of this licence, visit http://creativecommons.org/licenses/by/4.0/.

References

Ali HRH, Hassan AI, Hassan YF, El-Wekil MM (2019) Colorimetric and fluorimetric (dual-mode) nanoprobe for the determination of pyrogallol based on the complexation with copper(II)- and nitrogen-doped carbon dots. Microchim Acta 186(12):850. https://doi.org/10.1007/s00604-019-3892-9

Ali HRH, Hassan AI, Hassan YF, El-Wekil MM (2021) Mannitol capped magnetic dispersive micro-solid-phase extraction of polar drugs sparfloxacin and orbifloxacin from milk and water samples followed by selective fluorescence sensing using boron-doped carbon quantum dots. J Environ Chem Eng 9(2):105078. https://doi.org/10.1016/j.jece.2021.105078

Ali MFB, Saraya RE, El Deeb S, Ibrahim AE, Salman BI (2023) An innovative polymer-based electrochemical sensor encrusted with Tb nanoparticles for the detection of favipiravir: a potential antiviral drug for the treatment of COVID-19. Biosensors 13(2):243. https://doi.org/10.3390/bios13020243

Bae WK, Char K, Hur H, Lee S (2008) Single-step synthesis of quantum dots with chemical composition gradients. Chem Mater 20(2):531–539. https://doi.org/10.1021/cm070754d

Branch SK (2005) Guidelines from the International Conference on Harmonisation (ICH). J Pharm Biomed Anal 38(5):798–805. https://doi.org/10.1016/j.jpba.2005.02.037

Choi Y, Thongsai N, Chae A, Jo S, Kang EB, Paoprasert P, Park SY, In I (2017) Microwave-assisted synthesis of luminescent and biocompatible lysine-based carbon quantum dots. J Ind Eng Chem 47:329–335. https://doi.org/10.1016/j.jiec.2016.12.002

Eskalen H, Uruş S, Cömertpay S, Kurt AH, Özgan Ş (2020) Microwave-assisted ultra-fast synthesis of carbon quantum dots from linter: Fluorescence cancer imaging and human cell growth inhibition properties. Ind Crops Prod 147:112209. https://doi.org/10.1016/j.indcrop.2020.112209

Ge B, Li Z, Xie Y, Yang L, Wang R, Chang J (2015) Determination of tigecycline by quantum dots/gold nanoparticles-based fluorescent and colorimetric sensing system. Curr Nanosci 11(2):206–213. https://doi.org/10.2174/1573413711666141219215710

Ghosh S, Gul AR, Park CY, Xu P, Baek SH, Bhamore JR, Kim MW, Lee M, Kailasa SK, Park TJ (2021) Green synthesis of carbon dots from Calotropis procera leaves for trace level identification of isoprothiolane. Microchem J 167:106272. https://doi.org/10.1016/j.microc.2021.106272

Hammad MA, Omar MA, Salman BI (2017) Utility of Hantzsch reaction for development of highly sensitive spectrofluorimetric method for determination of alfuzosin and terazosin in bulk, dosage forms and human plasma. Luminescence 32(6):1066–1071. https://doi.org/10.1002/bio.3292

Honeyman L, Ismail M, Nelson ML, Bhatia B, Bowser TE, Chen J, Mechiche R, Ohemeng K, Verma AK, Cannon EP, Macone A, Tanaka SK, Levy S (2015) Structure-activity relationship of the aminomethylcyclines and the discovery of omadacycline. Antimicrob Agents Chemother 59(11):7044–7053. https://doi.org/10.1128/AAC.01536-15

Hussein ZF (2013) Study the effect of eruca sativa leaves extract on male fertility in albino mice. J Al-Nahrain Univ 16(1):1–8

Ji AJ, Saunders JP, Amorusi P, Wadgaonkar ND, O'Leary K, Leal M, Dukart G, Marshall B, Fluhler EN (2008) A sensitive human bone assay for quantitation of tigecycline using LC/MS/MS. J Pharm Biomed Anal 48(3):866–875. https://doi.org/10.1016/j.jpba.2008.06.020

Ji Ji A, Saunders JP, Amorusi P, Stein G, Wadgaonkar ND, O'Leary KP, Leal M, Fluhler EN (2010) Determination of tigecycline in human skin using a novel validated LC–MS/MS method. Bioanalysis 2(1):81–94. https://doi.org/10.4155/bio.09.159

Jothi VK, Ganesan K, Natarajan A, Rajaram A (2021) Green synthesis of self-passivated fluorescent carbon dots derived from rice bran for degradation of methylene blue and fluorescent ink applications. J Fluoresc 31(2):427–436. https://doi.org/10.1007/s10895-020-02652-6

Larsson MA, Ramachandran P, Jarujamrus P, Lee HL (2022) Microwave synthesis of blue emissive N-doped carbon quantum dots as a fluorescent probe for free chlorine detection. Sains Malaysiana 51(4):1197–1212. https://doi.org/10.17576/jsm-2022-5104-20

Magalhães da Silva L, Emilia de Almeida A, Salgado RN (2012) Thermal analysis and validation of UV and visible spectrophotometric methods for the determination of new antibiotic tigecycline in pharmaceutical product. Adv Anal Chem Sci Acad Publ 2(1):10–15. https://doi.org/10.5923/j.aac.20120201.03

Magdy G, Said N, El-Domany RA, Belal F (2022) Nitrogen and sulfur-doped carbon quantum dots as fluorescent nanoprobes for spectrofluorimetric determination of olanzapine and diazepam in biological fluids and dosage forms: application to content uniformity testing. BMC Chem 16(1):98. https://doi.org/10.1186/s13065-022-00894-y

Milosavljevic V, Nguyen HV, Michalek P, Moulick A, Kopel P, Kizek R, Adam V (2015) Synthesis of carbon quantum dots for DNA labeling and its electrochemical, fluorescent and electrophoretic characterization. Chem Papers. https://doi.org/10.2478/s11696-014-0590-2

Miyazawa M, Maehara T, Kurose K (2002) Composition of the essential oil from the leaves of *Eruca sativa*. Flavour Fragr J 17(3):187–190. https://doi.org/10.1002/ffj.1079

Molina-García L, Llorent-Martínez EJ, Ortega-Barrales P, Fernández-de Córdova ML, Ruiz-Medina A (2011) Photo-chemically induced fluorescence determination of tigecycline by a stopped-flow multicommutated flow-analysis assembly. Anal Lett 44(1–3):127–136. https://doi.org/10.1080/00032719.2010.500772

Neriman TB, Mehmet EI, Mahmut T (2011) Mineral content of the rocket plant (*Eruca sativa*). Afr J Biotech 10(64):14080–14082. https://doi.org/10.5897/AJB11.2171

Omar MA, Hammad MA, Salman BI, Derayea SM (2016) Highly sensitive spectrofluorimetric method for determination of doxazosin through derivatization with fluorescamine; Application to content uniformity testing. Spectrochim Acta a Mol Biomol Spectrosc 157:55–60. https://doi.org/10.1016/j.saa.2015.12.012

Salman BI (2023) A novel design eco-friendly microwave-assisted Cu–N@CQDs sensor for the quantification of eravacycline via spectrofluorimetric method; application to greenness assessments, dosage form and biological samples. J Fluorescence. https://doi.org/10.1007/s10895-023-03190-7

Salman BI, Ali MFB, Marzouq MA, Hussein SA (2019) Utility of the fluorogenic characters of benzofurazan for analysis of tigecycline using spectrometric technique; application to pharmacokinetic study, urine and pharmaceutical formulations. Luminescence 34(2):175–182. https://doi.org/10.1002/bio.3590

Salman BI, Hassan AI, Hassan YF, Saraya RE (2022a) Ultra-sensitive and selective fluorescence approach for estimation of elagolix in real human plasma and content uniformity using boron-doped carbon quantum dots. BMC Chem 16(1):58. https://doi.org/10.1186/s13065-022-00849-3

Salman BI, Hassan YF, Ali MFB, Batakoushy HA (2023) Ultrasensitive green spectrofluorimetric approach for quantification of Hg(II) in environmental samples (water and fish samples) using cysteine@MnO_2 dots. Luminescence 38(2):145–151. https://doi.org/10.1002/bio.4431

Salman BI, Hassan YF, Eltoukhi WE, Saraya RE (2022b) Quantification of tyramine in different types of food using novel green synthesis of ficus carica quantum dots as fluorescent probe. Luminescence 37(8):1259–1266. https://doi.org/10.1002/bio.4291

Salman BI, Ibrahim AE, el Deeb S, Saraya RE (2022c) Fabrication of novel quantum dots for the estimation of COVID-19 antiviral drug using green chemistry: application to real human plasma. RSC Adv 12(26):16624–16631. https://doi.org/10.1039/d2ra02241a

Saraya RE, el Deeb S, Salman BI, Ibrahim AE (2022) Highly sensitive high-performance thin-layer chromatography method for the simultaneous determination of molnupiravir, favipiravir, and ritonavir in pure forms and pharmaceutical formulations. J Sep Sci 45(14):2582–2590. https://doi.org/10.1002/jssc.202200178

Villano S, Steenbergen J, Loh E (2016) Omadacycline: development of a novel aminomethylcycline antibiotic for treating drug-resistant bacterial infections. Future Microbiol 11(11):1421–1434. https://doi.org/10.2217/fmb-2016-0100

Wang X, Feng Y, Dong P, Huang J (2019) A mini review on carbon quantum dots: preparation, properties, and electrocatalytic

application. Front Chem. https://doi.org/10.3389/fchem.2019.00671

Yang W, Yang H, Ding W, Zhang B, Zhang L, Wang L, Yu M, Zhang Q (2016) High quantum yield ZnO quantum dots synthesizing via an ultrasonication microreactor method. Ultrason Sonochem 33:106–117. https://doi.org/10.1016/j.ultsonch.2016.04.020

Zimmer D (2014) New US FDA draft guidance on bioanalytical method validation versus current FDA and EMA guidelines: chromatographic methods and ISR. Bioanalysis 6(1):13–19. https://doi.org/10.4155/bio.13.298

Publisher's Note Springer Nature remains neutral with regard to jurisdictional claims in published maps and institutional affiliations.